Understanding mixed-mode cyclic fatigue delamination growth in unidirectional composites

An experimental approach

Amaral, Lucas; Alderliesten, René; Benedictus, Rinze

DOI
10.1016/j.engfracmech.2017.05.049

Publication date
2017

Document Version
Accepted author manuscript

Published in
Engineering Fracture Mechanics

Postprint of Engineering Fracture Mechanics
Volume 180, July 2017, Pages 161-178
Link to formal publication (Elsevier): https://doi.org/10.1016/j.engfracmech.2017.05.049

Understanding Mixed-Mode Cyclic Fatigue Delamination Growth in unidirectional composites: an experimental approach

Lucas Amaral*, René Alderliesten, Rinze Benedictus

Structural Integrity & Composites Group, Faculty of Aerospace Engineering, Delft University of Technology, Kluyverweg 1, 2629HS Delft, The Netherlands

*Corresponding author at: Structural Integrity & Composites Group, Faculty of Aerospace Engineering, Delft University of Technology, Kluyverweg 1, 2629HS Delft, The Netherlands.
E-mail address: L.Amaral@tudelft.nl

Abstract

Due to the lack of fundamental knowledge of the physics behind delamination growth, certification authorities currently require that composite structures in aircraft are designed such that any delamination will not grow. This usually leads to an overdesign of the structure, hampering weight reductions. In real structures, delaminations tend to grow under a mix of modes I and II. Although some studies have tried to assess mixed-mode fatigue delamination, little progress was made in understanding the physics behind the problem. Therefore, this work scrutinizes mixed-mode fatigue delamination growth and examines experimentally the damage mechanisms that lead to fracture. To this aim, mixed-mode delamination fatigue tests were performed at different mode mixities, displacement ratios and maximum displacements. Selected fracture surfaces were analysed after the tests in a Scanning Electron Microscope to gain insight on the damage mechanisms. The physical Strain Energy Release Rate G^* was used as the similitude parameter, enabling the characterization of fatigue mixed-mode delamination propagation. The results obtained show no displacement ratio or maximum displacement dependence. Furthermore, the energy dissipated per area of crack created is approximately constant for a given mode mixity. However, the analyses of the fracture surfaces and the correlation of the damage features with energy dissipation indicate that different damage mechanisms that might be activated under different loading parameters cause the resistance to delamination to change under a given loading mode.

1. Introduction

The use of composite materials has enabled the design of lighter aircraft structures. However, laminated composites have poor interlaminar strength [1], which causes delaminations to be the most frequently observed damage mode in Carbon Fibre Reinforced Polymer (CFRP) structures [2]. The models currently used to assess delamination growth are phenomenological in nature, relying on curve fittings of experimental data, and are not based on the physics of the problem [3]. Due to this lack of fundamental knowledge of the physics behind delamination growth, certification authorities currently require that composite structures in aircraft are designed such that any delamination will not grow [4]. This leads to

an overdesign of these structures, hampering a further weight reduction that would be possible if delaminations were allowed to grow to a certain size before repair. Therefore, understanding the physics behind delamination growth is the first step towards designing lighter load-bearing composite structures for aircraft.

In real structures, delaminations tend to grow under a mix of modes I and II [5]. Although some studies have tried to assess mixed-mode fatigue delamination, little progress was made in understanding the physics behind the problem. In [4, 6], authors identified a stress ratio dependence in mixed-mode fatigue delamination tests, being the stress ratio defined as the ratio between minimum and maximum load, $R_\sigma=P_{min}/P_{max}$. Meanwhile Zhang et al. [7] showed that the Paris curves shift when tests are performed with different maximum displacements while keeping the stress ratio constant. None of them presented explanations for these observations. In fact, one should note that the effect of the stress ratio in energy dissipation during fatigue damage growth is a phenomenon controlled by two parameters. These parameters are, namely, the cyclic work and the maximum work applied. This is illustrated in Figure 1, which shows 3 different constant amplitude displacement controlled fatigue cycles. Let the displacement ratio be defined as the ratio between minimum and maximum applied displacements, $R_\delta=\delta_{min}/\delta_{max}$. The concept of using the ratio between minimum and maximum displacements is because R_δ is constant in displacement controlled tests. This was also used by Zhang et al. [7]. Loading cycles A and B have different displacement ratios but share the same maximum displacement. Therefore, the energy dissipated in a given increment of crack growth *da* might be the same for loading cycles A and B. Meanwhile, loading cycles A and C have the same displacement ratio and different maximum displacements, and they dissipate a different amount of energy per crack increment *da*. Therefore, in order to study the effect of the displacement ratio in energy dissipation, both cyclic energy and maximum work applied, i.e. displacement ratio and maximum displacement, must be considered. Studies that reported a stress ratio dependence [4, 6] did not report if the maximum work applied was changed when changing the stress ratio. On the other hand, the study in which Zhang et al. [7] observed differences in energy dissipation when changing the maximum displacement was performed only in one displacement ratio. Effectively, no studies were found in which the effects of different displacement ratios and maximum applied work were simultaneously investigated in a range of mode mixities.

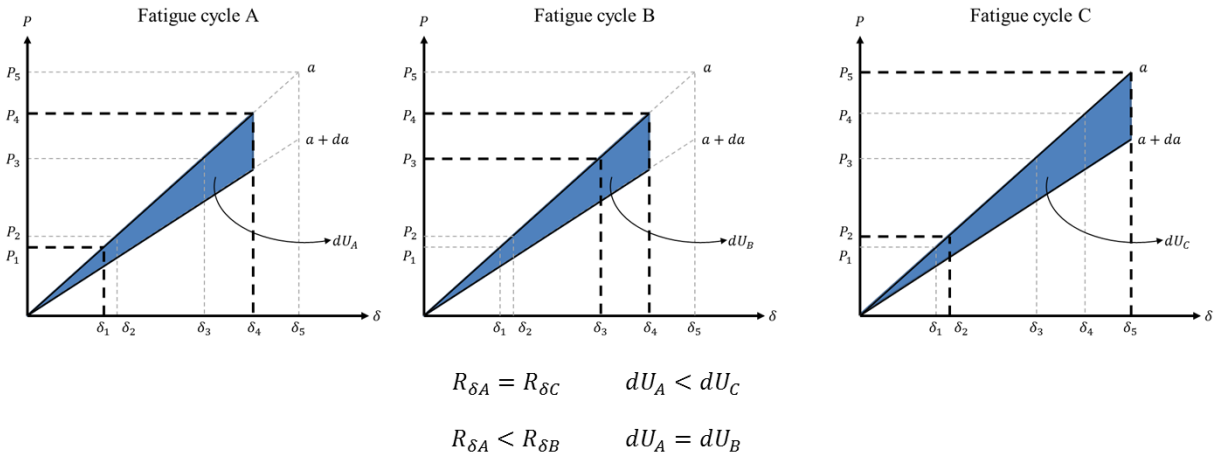

Figure 1. Illustration shows that constant amplitude fatigue cycles with different displacement ratios might have the same energy dissipation for a given crack increment *da*

Moreover, studies available in literature, such as [4, 6-10], often focused on simply obtaining phenomenological power-law relations in order to best fit the data. In some of these studies [4, 6, 7], no fracture surfaces were examined, hindering the understanding of the damage mechanisms and the physics of delamination growth. Some authors [8-10], however, report both empirical models and analysis of fracture surfaces. In particular, Asp et al. [10] related the damage mechanisms acting in fracture propagation to the calculated Strain Energy Release Rate (SERR) levels. However, the use of different similitude principles when assessing fatigue delamination misleads the interpretation of the results [11]. No agreement has been reached on which parameter should be used to describe similitude appropriately for the assessment of fatigue delamination growth [3, 12]. Some authors use the maximum SERR G_{max} [13], while others prefer the SERR range $\Delta G = G_{max} - G_{min}$ [14], although $\Delta\sqrt{G} = (\sqrt{G_{max}} - \sqrt{G_{min}})^2$ was pointed out as a parameter that correctly applies the similarity principle [11, 12]. None of these parameters, however, describes uniquely a load cycle, which also leads to the observation of a stress ratio dependence [3]. In addition, these parameters describe an artificial SERR that can be calculated even when there is no crack growth. This concept of SERR has been developed assuming fixed grip conditions that do not apply during fatigue loading [15, 16].

In an effort to solve this problem, the work performed in [15-21] is noteworthy. In these papers, a physical SERR G^*, which is derived from combining applied work with crack extension throughout the fatigue test, is used to characterize fatigue crack growth. The use of this physical SERR has enabled a better understanding of the physics underlying delamination growth. Moreover, the physical SERR enabled the correlation of the fracture surfaces generated in crack extension with the actual energy dissipated in this crack growth.

1.1.Problem Statement and Research Objectives

Mixed-mode fatigue delamination is not well understood. This is demonstrated by the fact that there is no consensus on displacement ratio dependence, the effects of the maximum load applied in the fatigue cycle, or even on the parameter describing the similitude. Furthermore,

do damage mechanisms change with a different stress ratio? What different damage features are observed on the fracture surface when the maximum load changes? The lack of appropriate answers to these questions are evidences of the gap between the way the macroscopic behaviour and the damage mechanisms acting in fracture are described. Although empirical delamination growth models based on curve fitting may help to provide quicker input for engineering predictions, they do not lead to understanding the physics underlying the observed phenomena. This is a common drawback of assessing problems with phenomenological empirical relations, which can fit very well the data, but provide no insight on why data behave as such. The fundamental understanding of fatigue delamination growth could set the path towards a design philosophy that relaxes the current "no growth" approach, resulting in a further weight reduction of aircraft.

Therefore, the aim of this work is to scrutinize mixed-mode fatigue delamination growth and examine experimentally the damage mechanisms that lead to fracture. Through that, this work seeks to understand the effects of different displacement ratios and maximum applied loads to fatigue delamination growth under different mode mixities, and provide physical explanations to it. In addition, the appropriateness of the term "stress ratio effect" for fatigue crack growth is discussed.

Following the use of the physical SERR G^* for interpreting mode I and mode II delamination and disbond growth [17-21], this parameter is employed here to characterize mixed-mode fatigue delamination growth. Besides, Scanning Electron Microscopy (SEM) is used to examine the fracture surfaces and gain insight on the damage mechanisms present at the fracture surfaces.

2. Methodology

2.1. Relating applied work to energy dissipation

The current paper uses the SERR as the correct approach to describe the similitude in fatigue damage growth. The reasoning, discussed in detail by Alderliesten [16] and summarized here, is that cyclic work is applied when fatigue loading a certain structure. Consider a brittle material system, where plasticity effects are negligible. In a similar manner to what Griffith proposed [22], a single fatigue cycle under displacement controlled conditions can be written in terms of energy

$$U_0 + U_{\uparrow} \rightarrow U_0^* + U_{\downarrow} + U_a \qquad (1)$$

where U_0 is the monotonic elastic strain energy available, $U_{\uparrow}$ is the work applied by the machine during loading, $U_{\downarrow}$ is the work applied by the machine during unloading and U_a is the energy dissipated in damage growth. These energies correspond to the areas below the curves illustrated in Figure 2.

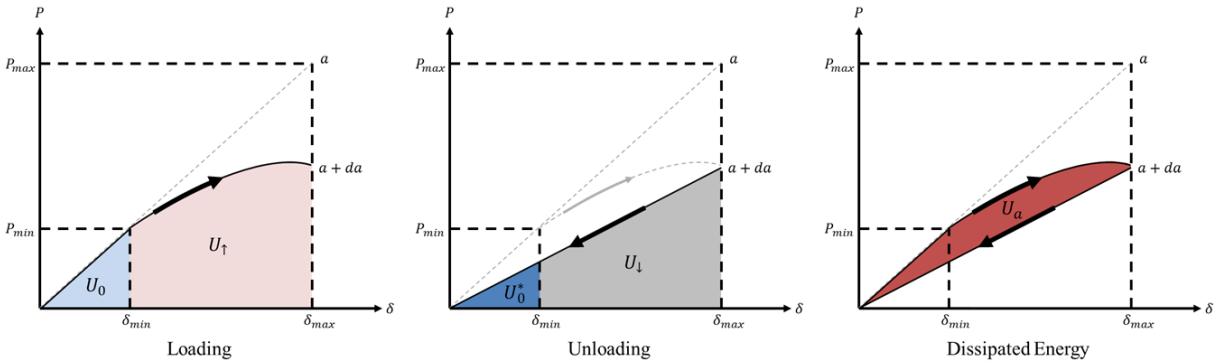

Figure 2. Applied work and energy dissipation in a single constant amplitude displacement controlled fatigue cycle

The difference between $U_\uparrow$ and $U_\downarrow$ is difficult to measure for a single load cycle. An approximate solution is to measure the elastic work applied to the structure at any load cycle $U_{N=i}$, where $U=½P\delta$, with P and δ the applied force and displacement, respectively. For the displacement controlled tests performed, the strain energy available will decrease with the number of cycles, such that the variation of the applied work can be easily calculated as dU/dN. Energy dissipation may occur in any load cycle, such that

$$U_0 + U_\uparrow \rightarrow U_0^* + U_\downarrow + dU/dN \quad (2)$$

The energy dissipated per cycle can be written as

$$dU/dN = (dU/dA)(dA/dN) \quad (3)$$

Note that the complete load cycle is included in the formulation of Eq. (2). The stress ratio has a similar effect on dU and da for a given cycle. Hence, Eq. (3) in which dU/dN and da/dN are plotted against each other may not exhibit a stress ratio effect as observed in Paris-type relationships [16].

The resistance to crack growth, which is the energy dissipated per area of crack created, dU/dA, can be obtained if the strain energy variation and the damage growth rate are measured throughout a test. This is illustrated in Figure 3. The reader should note that, according to Eq. (3), dU/dA is calculated plotting a straight line from the origin of the coordinate system to each data point. The inclination of each of the straight lines obtained between the origin and the data point is $1/(dU/dA)$. Energy dissipation per area of crack, dU/dA, was observed to increase with an increasing crack growth rate for mode I delaminations [15, 16]. The higher the crack growth rate, the closer to quasi-static fracture the process is. The closer a fracture is to quasi-static, the more energy is dissipated per area, because quasi-static fracture is less energetically efficient than fatigue fracture. This relates to the damage mechanisms observed on the fracture surfaces. With an increase in the crack growth rate, more damage features and different damage mechanisms were encountered on the fracture surface, responsible for the aforementioned increase in energy dissipation [15].

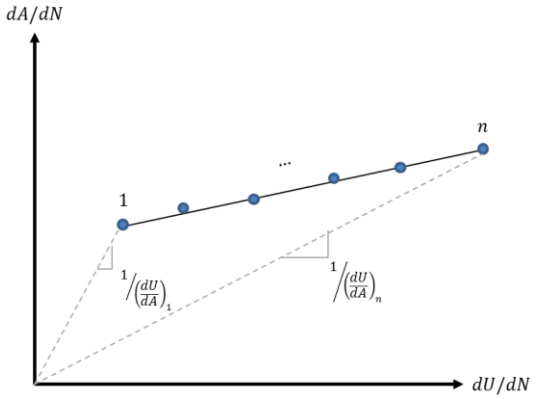

Figure 3. Determining the energy dissipated per area of crack created: resistance to crack growth increases with the crack growth rate

2.2. The Mixed-Mode Bending Test

The Mixed-Mode Bending (MMB) test fixture, schematically illustrated in Figure 4 (a), was used to load split specimens at different ratios of Mode I to Mode II loading, where *Wg* is the centre of gravity of the lever-yoke assembly, *cg* is the lever length to the centre of gravity and *c* is the lever length of the MMB test apparatus. The mode mixity, defined as

$$G_{II}/G=G_{II}/(G_I + G_{II}) \quad (4)$$

is kept constant throughout all tests. In total, 38 specimens were fatigue tested at different stress ratios under constant amplitude, displacement controlled conditions. Tests were performed at different maximum displacements, in order to understand the effect of the maximum applied load on energy dissipation in fatigue delamination growth. The test matrix is presented on Table 1.

Table 1. Test Matrix

Number of tests	$(\delta_{max}/\delta_{crit})$	**R**	(G_{II}/G)
3	0.75	0.1	0.20
2	0.85		
3	0.90		
3	0.75	0.5	
3	0.85		
4	0.90		
2	0.85	0.7	
3	0.85	0.1	0.50
3	0.85	0.5	
3	0.85	0.7	
3	0.88	0.1	0.80
3	0.88	0.5	
3	0.88	0.7	

The results of constant amplitude, displacement controlled Double Cantilever Beam (DCB) and End-Notched Flexure (ENF) fatigue tests for the same material, discussed in [17, 20], are also used at the present work.

2.3. Material and specimen preparation

Unidirectional laminates were manufactured with 32 layers of Carbon Fibre Reinforced Epoxy prepreg from the same material batch, M30SC-150-DT 120-34F. The prepreg is manufactured by Delta Tech. The product was cured in an autoclave following the cure cycle recommended by the manufacturer. A 13 μm thick Polytetrafluorethylene (PTFE) film was placed in the middle layer as the crack starter. The cured laminates were C-scanned to ensure that they were free of defects, using a panel made of the same material with voids of approximately *1 mm* diameter as reference. *25 mm* wide specimens were cut from the laminates using a waterjet cutting machine according to the dimensions shown in Figure 4 (b). End blocks were bonded to the specimens for load introduction following the guidelines given in ASTM Standard D 6671 [23]. A camera was positioned alongside the specimen during the test and crack length measurement was performed in a post-test analysis of the pictures taken, using an open-source image analysis software, ImageJ. The pictures were taken using an Optomotive Velociraptor camera system. To aid in crack detection, the sides of the specimen were sanded and coated with a thin layer of white water-based typewriter correction fluid, and vertical pencil lines were drawn every *15 mm*, as shown in Figure 5.

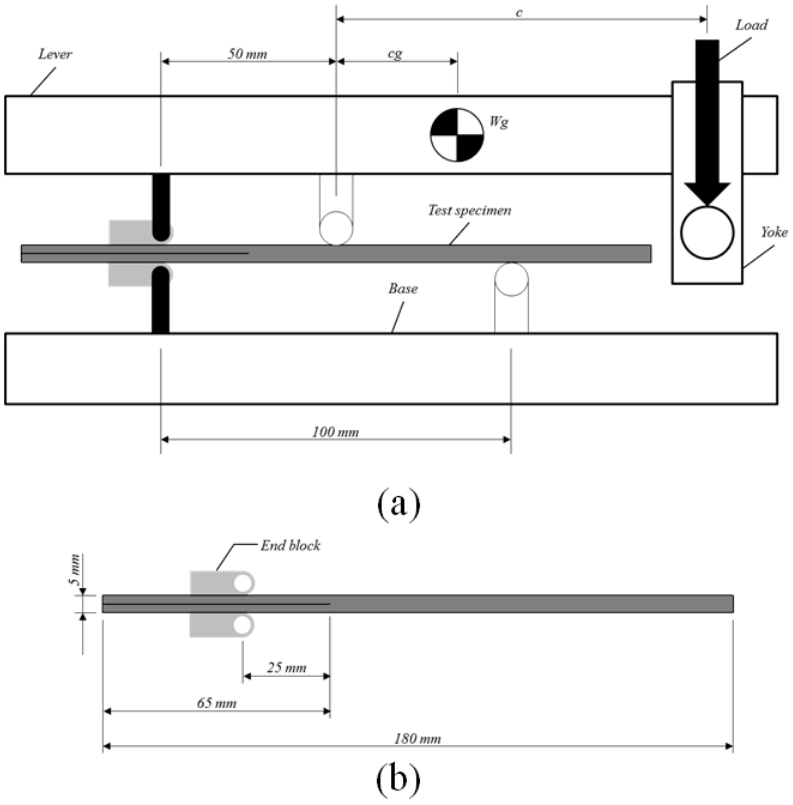

Figure 4. (a) MMB test fixture; (b) specimen dimensions

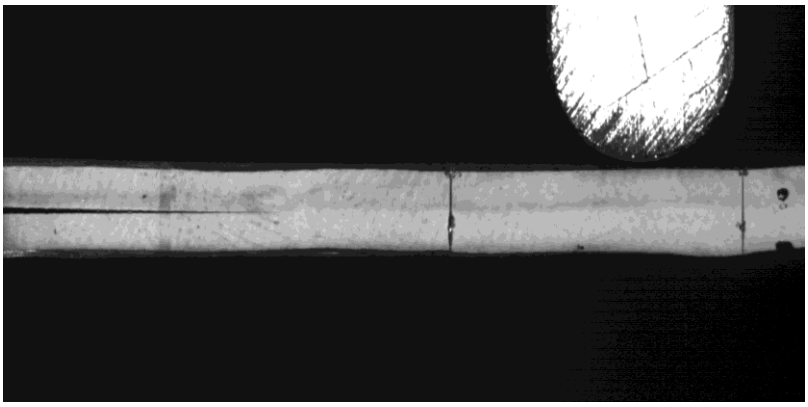

Figure 5. Crack detection

All tests were conducted in a MTS machine equipped with a *10 kN* load-cell. The test set-up was designed according to ASTM D6671 [23] and is shown in Figure 6. For the analysis performed in this work, which is under displacement controlled conditions, the rate of energy dissipation is calculated through the decrease in the applied work. The weight of the lever is constant, and so is its position for a given mode-mixity. Therefore, the lever weight does not influence in the calculation of the rate of energy dissipation, once this is performed taking the derivative of the decrease in applied work with the number of cycles. When performing a comparison between different mode-mixities, the position of the centre of gravity of the lever did not influence the results in a considerable manner. Both load and displacement were calibrated and had in the load-displacement ranges used in the tests a relative error of 0.86% and 1%, respectively. Table 2 shows the material data as obtained by Rodi [24], and the position of the yoke calculated according to the ASTM standard [23]. To gain insight into the damage mechanisms acting during fracture, 13 specimens were analysed in a Scanning Electron Microscope (SEM), after the tests were performed.

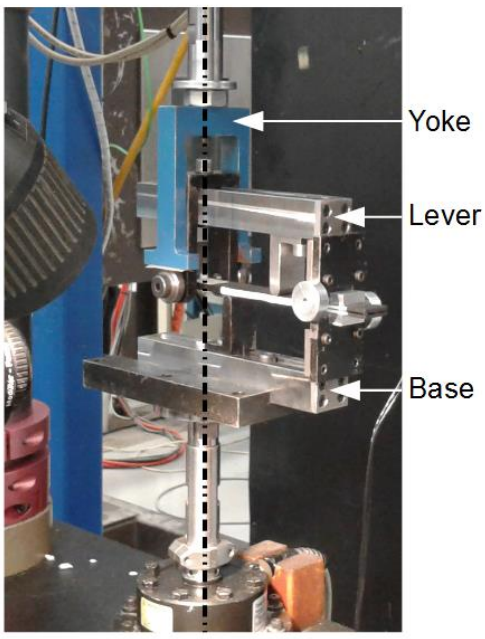

Figure 6. MMB apparatus during test

Table 2. (a) Positions on the test fixture; (b) Material data;

G_{II}/G	c mm	cg mm
20	90	43
50	40	28
80	27	24

(a)

Material Data	
E_{11} GPa	155
E_{22} GPa	7.8
G_{12} GPa	5.5

(b)

2.4. Calculating the physical SERR *G**

The crack growth rate, *da/dN*, is calculated from the measured crack length throughout the test. Meanwhile, the rate of the average strain energy dissipated per cycle, *dU/dN*, is calculated from the potential strain energy measured throughout the test. First, the graphs of *a versus N* and *U versus N* are plotted, where *a* is the crack length, *U* is the potential strain energy of the system and *N* is the number of cycles. Considering linear elasticity, the potential strain energy is defined as $U=½P\delta_{max}$. However, due to the compliance of the test fixture, a small portion of nonlinearity is observed when the load goes from *0 N* to δ_{min}. In order to account for this nonlinearity, a correction is introduced, such that both δ_{max} and δ_{min} are used to calculate an approximated *U*, as shown in Figure 7.

The data points obtained are fitted by a seven point incremental polynomial function suggested by ASTM [25], and the rates of crack growth and energy dissipation are calculated from these polynomial fits. Being *b* the width of the specimen, the physical SERR *G** is then obtained from [17, 26]:

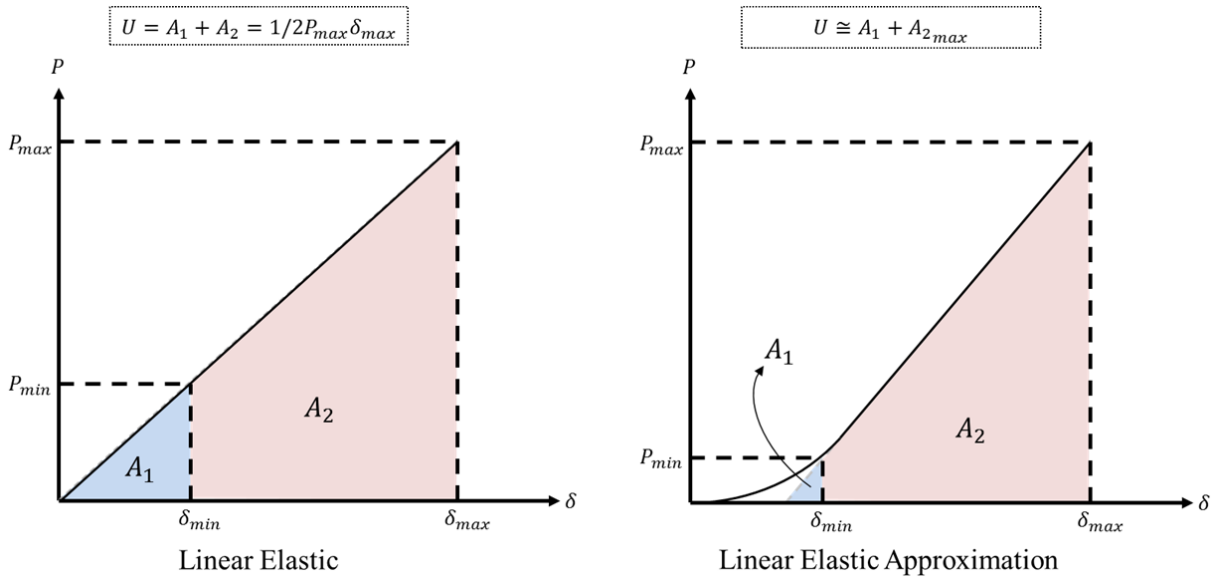

Figure 7. Approximation in the calculation of the potential strain energy due to the compliance of the test fixture

$$G^*=(1/b)*(dU/dN)/(da/dN)=dU/dA \quad (5)$$

3. Results and Discussion

The results obtained show no displacement ratio or maximum displacement dependence. Furthermore, *dU/dA* appears to be approximately constant throughout all fatigue tests performed, although tests at 80% of mode II loading seemingly show a bigger scatter at low crack growth rates. The results are presented in Figure 8. The correlations between energy dissipation per cycle and damage growth rate are shown in Figure 8 (a-c). The energy dissipation per area of crack created is correlated to damage growth rate in Figure 8 (d). Although the data is presented on a double logarithmic scale for clarity, each of the results in Figure 8 shows linear trends, also if one considers linear plots.

Each of these results is discussed in detail hereafter, starting with the behaviour observed in tests at 80% of mode II loading. When comparing the results for different mode mixities in Figure 8, obvious scatter is observed in the results of tests performed at 80% of mode II loading. The first question that is addressed here is: what is the physical explanation for this phenomenon?

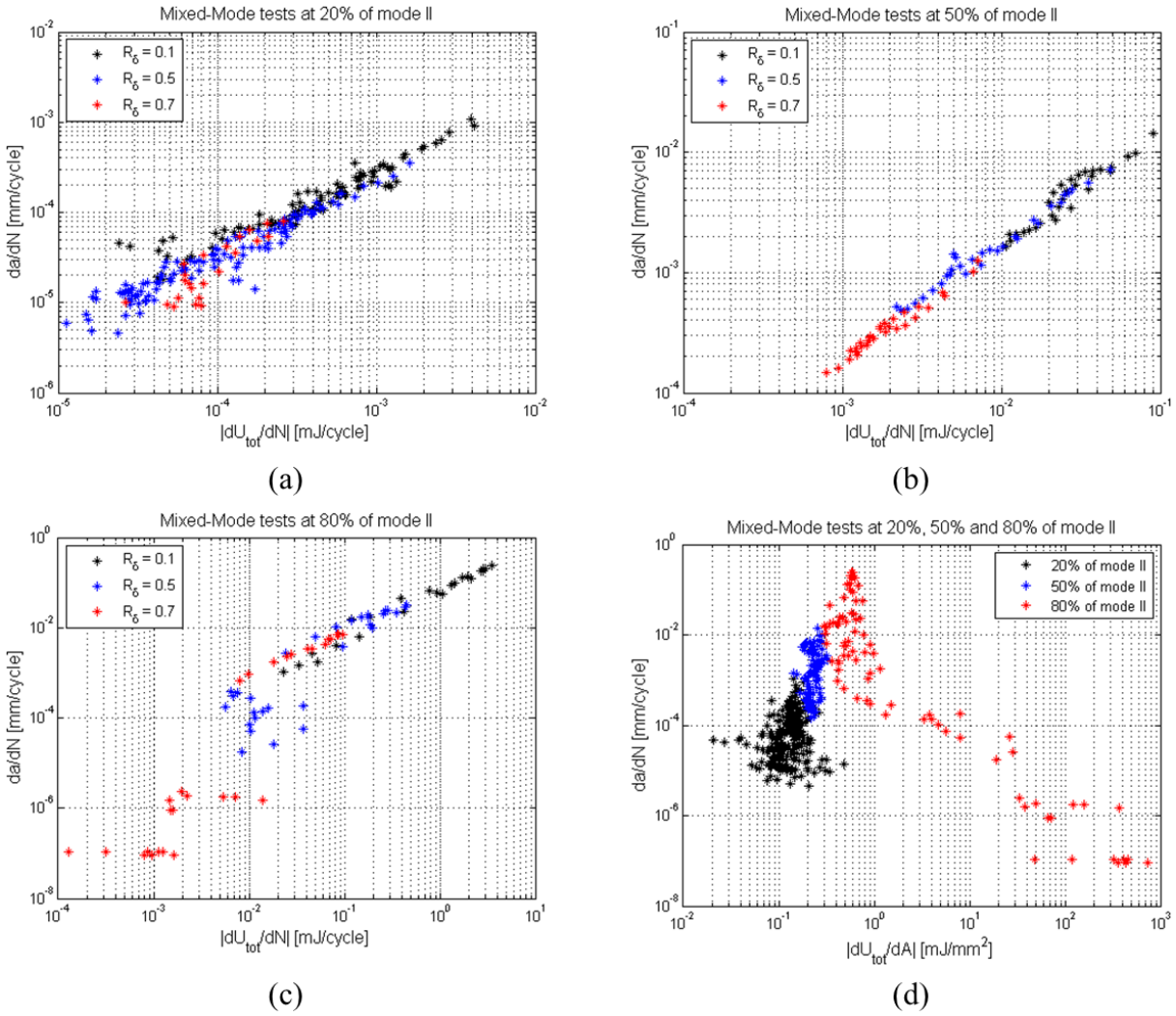

Figure 8. Mixed-mode fatigue tests performed at (a) 20% of mode II; (b) 50% of mode II; (c) 80% of mode II; (d) resistance to fatigue crack growth at 20%, 50% and 80% of mode II loading

3.1. Process zone effects on mode II dominated fracture

The behaviour observed for low crack growth rates in tests at 80% of mode II loading, shown in Figure 8 (c) and (d), is explained by the energy dissipated in the process zone ahead of the physical delamination tip [27]. In mode II delamination extension, a process zone develops with the formation of cusps, striations and microcracks ahead of the crack tip until coalescence is reached and crack growth can be observed from the sides of the specimen [10, 28-31]. These damage mechanisms dissipate a significant amount of energy which is unaccounted for when calculating the crack growth rate *da/dN*, since the damage on the process zone cannot be visualized and quantified. This causes an error when relating energy dissipation per cycle with crack growth rate. Such an error was shown to be significantly high for tests performed at high displacement ratios [17].

For tests performed at 80% of mode II and high displacement ratios, i.e., $R_\delta = 0.5$ and 0.7, the same behaviour described for pure mode II fatigue tests in [17] is observed. Figure 9 shows the crack length evolution throughout a fatigue test at $R_\delta = 0.5$ and a fracture surface of this test. The zone indicated by the red arrow in Figure 9 (a) shows slow crack growth. Afterwards, the crack grows faster until it is arrested at the location in the specimen underneath the bending load introduction.

The slow crack growth shown in Figure 9 (a) is accompanied with the development of the process zone, dissipating substantial strain energy that cannot be correlated to the rate of damage growth, *da/dN*. On the fracture surfaces corresponding to the areas of process zone development, such as in Figure 9 (b), cusps and cracks on the fibre imprints are abundantly observed [17]. Hence, G^* is calculated wrongly for moments when the process zone is developing at expense of crack growth. Meanwhile, the area with a fast crack growth corresponds to the coalescence of the damage ahead of the crack tip. In this phase, the energy dissipated can be approximately correlated with damage growth, because damage is mainly in the form of visible crack growth due to coalescence of the process zone. However, the measured energy dissipation *dU/dN* during fast crack growth is correlated to the formation of the entire cracked surface, and not only to the coalescence of the pre-existing damage ahead of the crack. Therefore, this consists on a first approximation, and the reader should be aware that the crack growth rate is, thus, overestimated in this case. To circumvent this problem, more research is necessary in order to understand the energy dissipated per area of crack created in the process zone of mode II dominated delaminations.

Because the physical SERR G^* cannot be calculated when the process zone development dominates damage growth, the crack growth data for these points in tests at $R_\delta = 0.5$ and 0.7 will not be considered in the results. Therefore, moments where process zone is developing, characterized by slow crack growth, such as in Figure 9 (a), will be omitted from the results. In a practical manner, this was established such that for tests at 80% of mode II loading, data points in which the crack increment was smaller than *0.1 mm* are omitted from now on in this paper. Figure 10 shows the correlations between energy dissipation and damage growth for different mode mixities after omitting the points in which process zone effects dominate fracture.

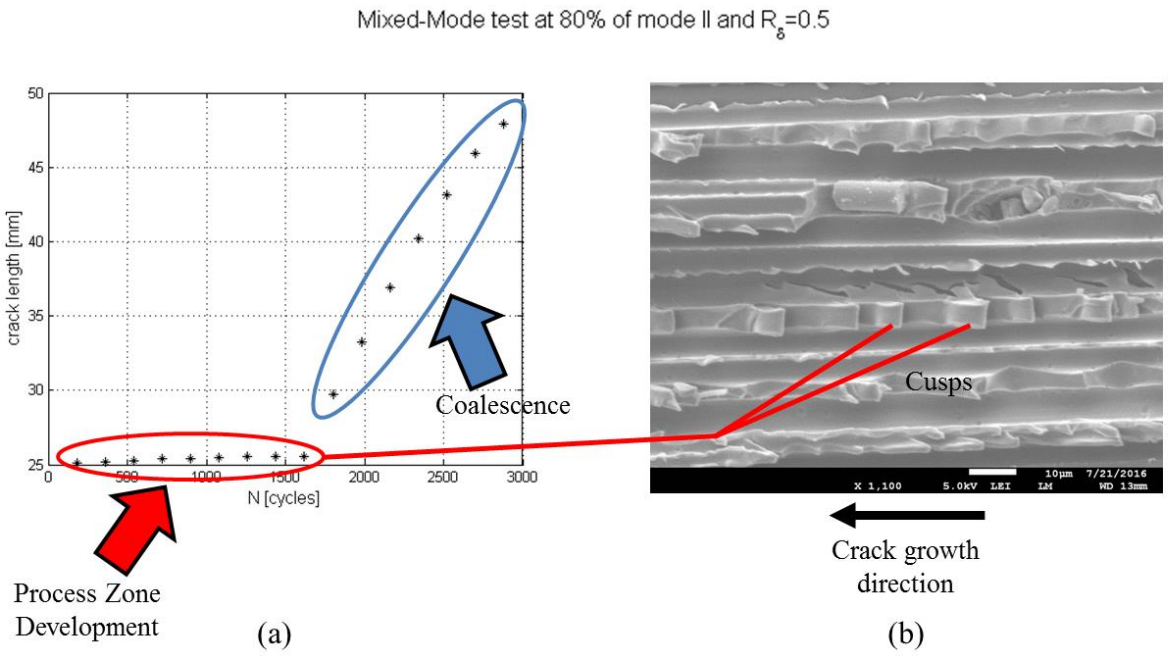

Figure 9. (a) Crack length evolution throughout the test shows effects of the process zone; (b) fracture surface of the corresponding fatigue test shows cusps developed

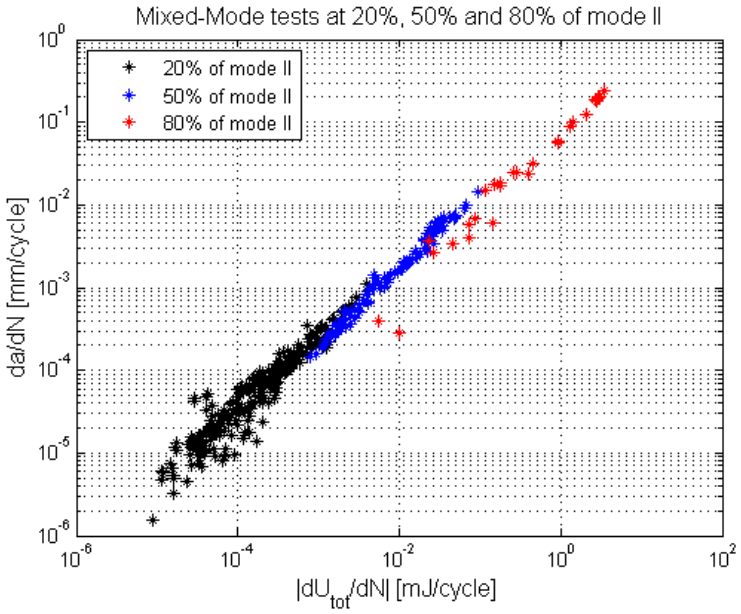

Figure 10. crack growth rate plotted against the energy dissipated per cycle – for 80% of mode II loading, crack increments smaller than *0.1 mm* were omitted

For tests performed at 20% and 50% of mode II loading, respectively, a smooth crack growth curve is observed in each of the tests, shown in Figure 11 (a) and (c). Figure 11 (b) and (d) shows fracture surfaces for these same tests. For the tests performed at 20% of mode II loading, fracture surfaces consist mostly of fibre imprints, brittle cleavage fracture and ribs, as exemplified in Figure 11 (b). Meanwhile, for tests performed at 50% of mode II loading, the fracture surfaces consist mostly of bare fibres, fibre imprints, more extensive matrix cleavage and some shallow cusps. Features that develop in the process zone, such as striations, deep

cracks on the fibre imprints and well-shaped cusps are not dominant on these fracture surfaces like they are on fracture surfaces of tests performed at 80% of mode II, exemplified in Figure 9 (b). Therefore, the energy dissipated in the process zone, which is not accounted for in the physical SERR G^*, is taken to be less extensive and to have limited influence in the results for fatigue mixed-mode delamination tests performed at 20% and 50% of mode II loading.

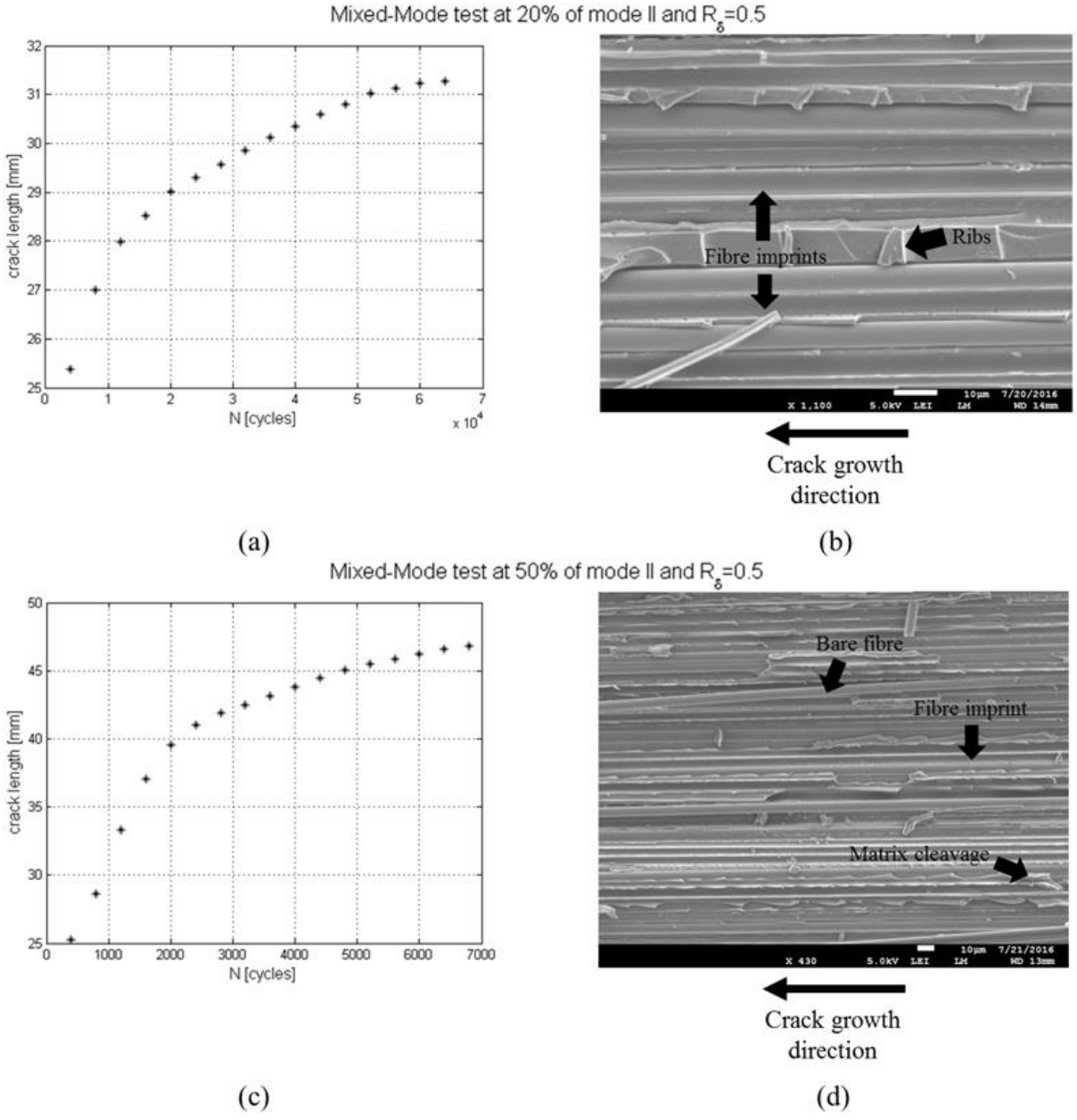

Figure 11. (a) crack growth throughout fatigue test at 20 % of mode II and $R_\delta = 0.5$ and (b) respective fracture surface; (c) crack growth throughout fatigue test at 50 % of mode II and $R_\delta = 0.5$ and (d) respective fracture surface;

3.2. The effects of the applied maximum displacement on delamination growth

Tests at 20% of mode II loading were performed with different maximum displacements and displacement ratios. The results are presented in Figure 12 (a-c) and show that damage growth rate and energy dissipation per cycle relate linearly. Furthermore, this linear relationship

aligns with the origin of the coordinate system, which indicates that the energy dissipated per area of crack created *dU/dA* is approximately constant, regardless of displacement ratio, maximum displacement and crack growth rate.

This behaviour, observed in Figure 12 (d), is counterintuitive. More energy is expected to be dissipated per area of crack created at higher crack growth rates, as discussed elsewhere [15]. However, such an increase in *dU/dA* is not obvious in the present study. This is due to the fact that for these tests, the damage mechanisms acting in delamination growth were observed to be approximately constant regardless of the applied peak displacement or displacement ratio in the examination of fracture surfaces. New dissipation mechanisms were not observed at higher values of *da/dN*. The main difference observed on the fracture surfaces was that, at higher crack growth rates, matrix presented higher deformation. However, resin deformation is then limited by matrix plasticity. Plasticity, which is logically expected to increase with the maximum displacement applied, is limited in this brittle material system. Therefore, its effects in energy dissipation are assumed to be negligible.

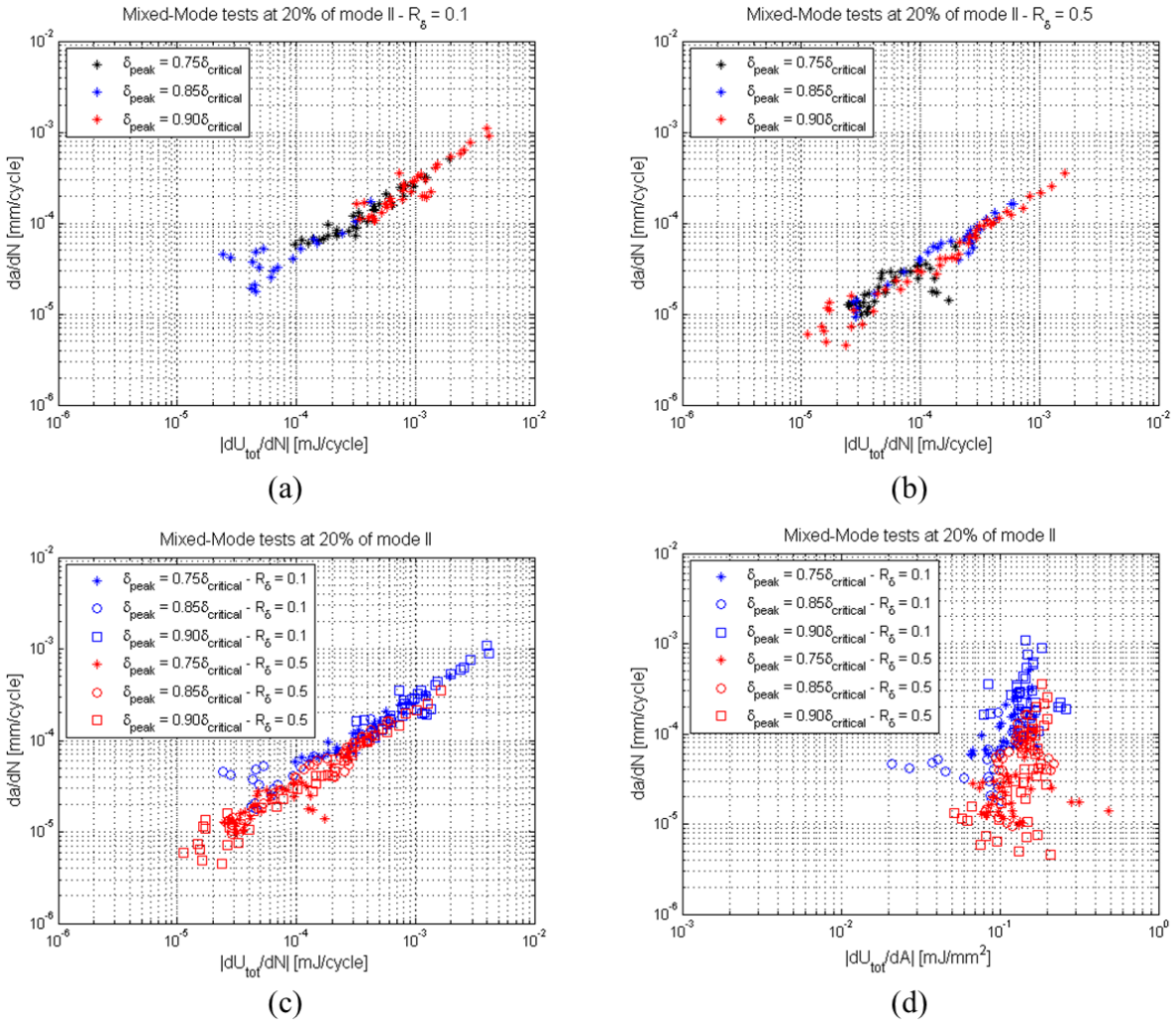

Figure 12. Effect of the maximum displacement: (a) tests performed at $R_\delta = 0.1$; (b) tests performed at $R_\delta = 0.5$; (c) all tests performed at 20% of mode II loading; (d) crack growth rate versus energy dissipated per area of crack created for all tests performed at 20% of mode II loading

A higher maximum displacement leads to a higher initial crack growth rate. Figure 13 presents fracture surfaces for tests at 20% of mode II under different crack growth rates. More matrix deformation can be observed for a higher crack growth rate, and the fracture surface looks less flat than for a low crack growth rate. This is the main difference between the fracture surfaces in Figure 13. However, as discussed above, the low level of plasticity limits the energy consumed by it in delamination growth. Because of this, an increase in *dU/dA* at higher crack growth rates is not obvious in Figure 12 (d), within the present scatter of data. Furthermore, for this material system, fatigue fracture at 20% of mode II loading consists basically of fibre pull-out leaving fibre imprints, ribs and some very shallow cusps. No significantly different damage mechanisms were observed at high crack growth rates. The same behaviour is observed for 50% of mode II loading, observed in Figure 14. The main difference between the fracture surfaces on Figure 14 is also that matrix deformation is more extensive on high crack growth rates, still falling into the case of limited plastic deformation.

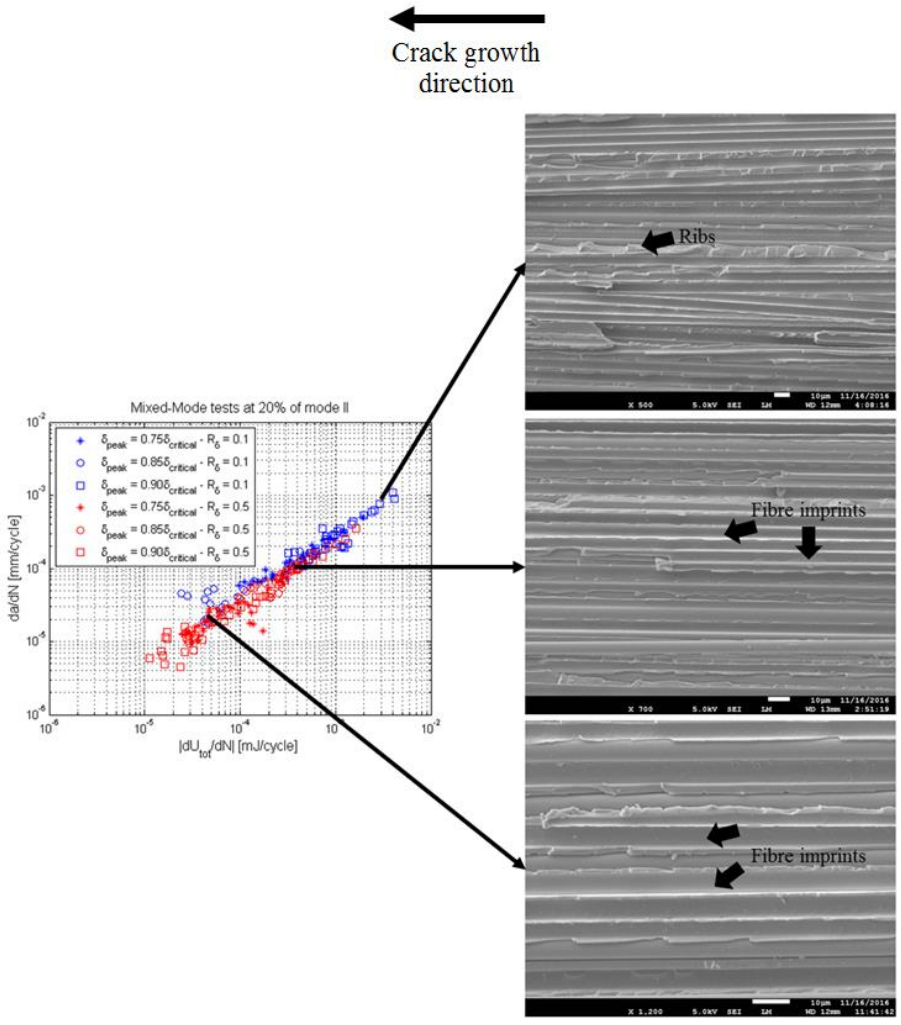

Figure 13. Data for 20% of mode II loading. In a higher crack growth rate, more area is created and proportionally more energy is dissipated to do this work, such that *dU/dA* is constant

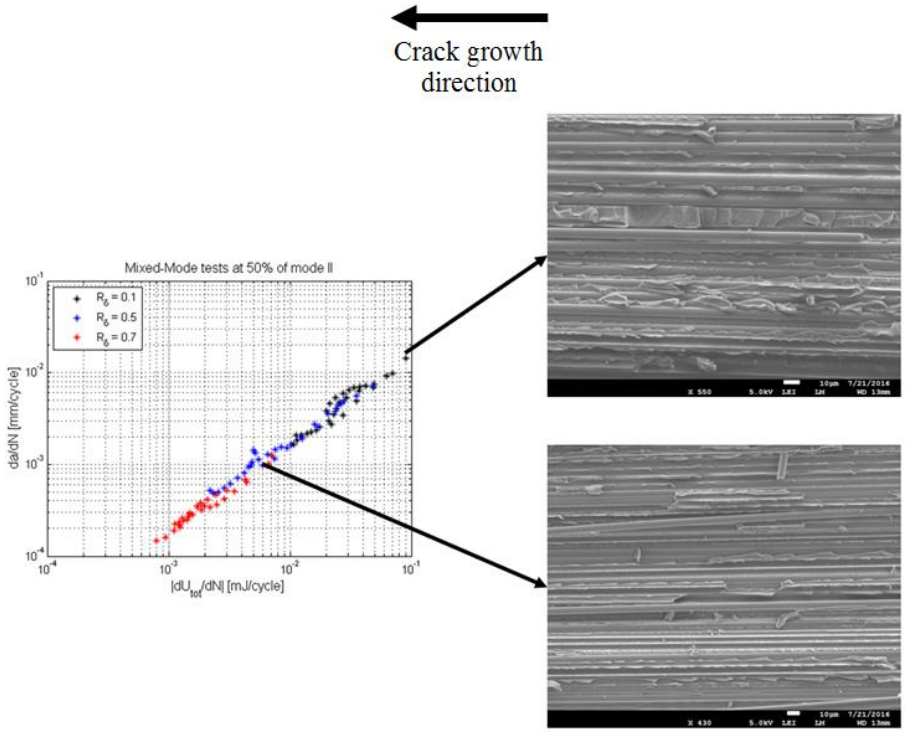

Figure 14. Data for 50% of mode II loading. In a higher crack growth rate, more area is created and proportionally more energy is dissipated to do this work, such that *dU/dA* is constant

3.3. Damage mechanisms: the key for understanding energy dissipation in fatigue delamination growth

The results of the present study show that damage mechanisms activated during fatigue loading determine the resistance to delamination growth. Consider Figure 15, which shows the results of the MMB fatigue tests performed. The relationship between crack growth rate and energy dissipation per cycle for each mode mixity in Figure 15 (a) has a linear relationship. Moreover, each of these linear relationships can be fitted by a straight line going through the origin with a correlation factor R^2 close to 1. This means that for a given mode mixity, the energy dissipated per area of crack created, $G^*=dU/dA$, is approximately constant. The discussion of section 3.2. applies to the whole dataset: this approximately constant behaviour of *dU/dA* is due to the fact that damage mechanisms encountered on the fracture surfaces for each mode mixity were constant independently of the crack growth rate.

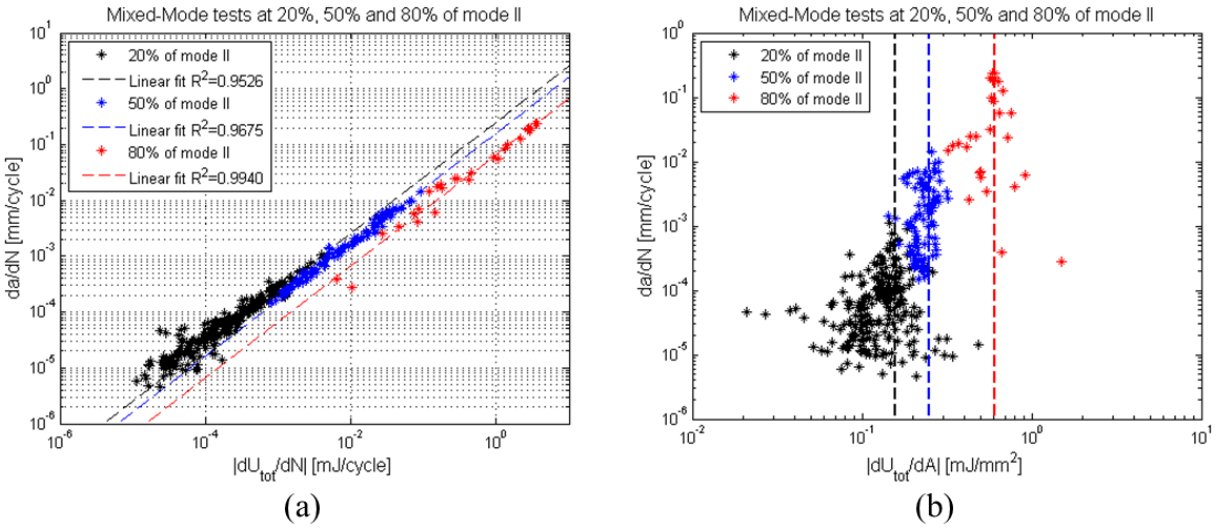

Figure 15. (a) relationship between crack growth rate and energy dissipation per cycle fitted with a straight line going through the origin of the coordinate system; (b) relationship between crack growth rate and delamination resistance for each mode mixity

In a similar manner, the relationship between different mode mixities can also be discussed from the perspective of damage mechanisms and energy dissipated in damage growth. Figure 15 (b) shows that each different percentage of mode II loading dissipates a different amount of energy per area of crack *dU/dA*. This occurs because each different mode of loading activates different damage mechanisms, and the energy dissipated to create a crack of area *dA* depends on the damage mechanisms acting in crack growth. The trendlines in Figure 15 (b) are simply obtained from the inclination of the trendlines fitted to the data in Figure 15 (a), also taking the width of the specimens into consideration. Figure 16 (a-c) shows typical damage mechanisms observed on fracture surfaces generated under 20%, 50% and 80% of mode II loading, respectively. For 20% of mode II loading, the main damage mechanisms observed were fibre pull-out, brittle matrix cleavage and the formation of ribs. For 50% of mode II loading more bare fibres are present, suggesting a more extensive interfacial failure. Furthermore, deformation of the matrix during cleavage fracture is more pronounced, ribs are less spaced between themselves and shallow cusps can also be encountered. Finally, for 80% of mode II loading, cusps and deep cracks on the fibre imprints are the mainly observed features, besides extensive matrix deformation. For each mode of loading, the only obvious change encountered on the fracture surfaces between high and low crack growth rates was in matrix deformation.

This suggests that, for delamination growth in unidirectional composites and a given mode of loading, there might be two main dissipation mechanisms that contribute to a substantial change on the resistance to delamination growth. The first consists of different damage mechanisms that might be activated under different fatigue loading parameters, such as higher maximum displacements. The second factor is the amount of energy dissipated by plasticity during matrix deformation. If the damage mechanisms acting during fracture remain approximately the same and other dissipation mechanisms, such as plasticity, are negligible, the energy that is dissipated per area of crack created can be approximated to be constant.

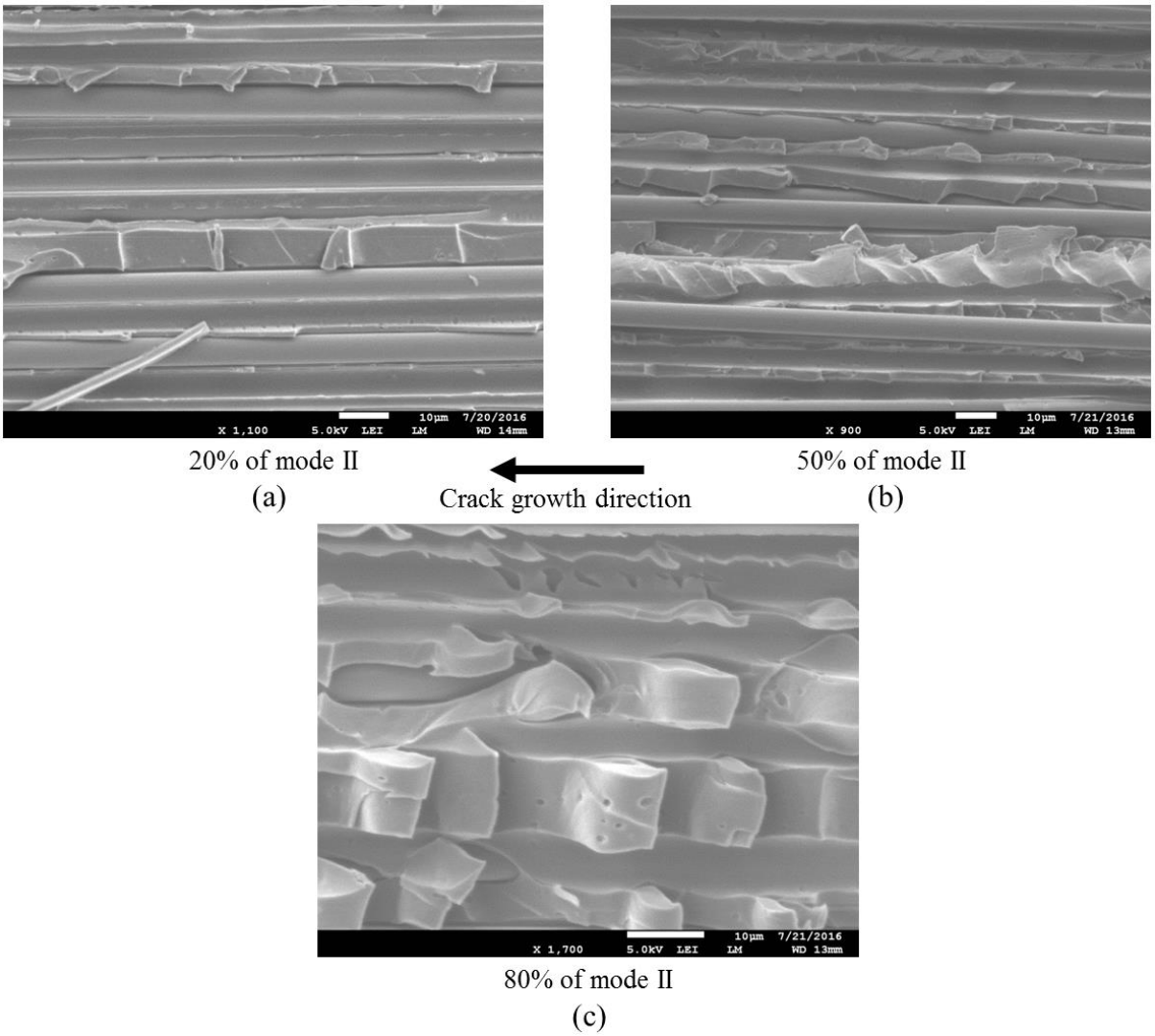

Figure 16. Typical damage mechanisms found in fracture surfaces for (a) 20% of mode II loading, (b) 50% of mode II loading and (c) 80% of mode loading

3.4. Breakage of bridging fibres: changing the damage mechanisms

An example of how different damage mechanisms can change the resistance to delamination growth can be observed in pure mode I DCB fatigue tests performed in the same material system, discussed in [20]. Figure 17 shows the correlations between mixed-mode and DCB fatigue tests for the same material. For a better visualization of the results, only the trends of the mixed-mode tests are plotted in Figure 17. Figure 17 (b) shows that the DCB data, for low crack growth rates, yield similar results to the ones obtained for mixed-mode tests at 20% of mode II loading. At a crack growth rate of approximately 10^{-4}*mm/cycle*, however, the DCB data seem to follow a different trend, and the resistance to delamination growth becomes similar to the one obtained for mixed-mode tests at 50% of mode II loading. The explanation behind this change in resistance is in the breakage of the bridging fibres.

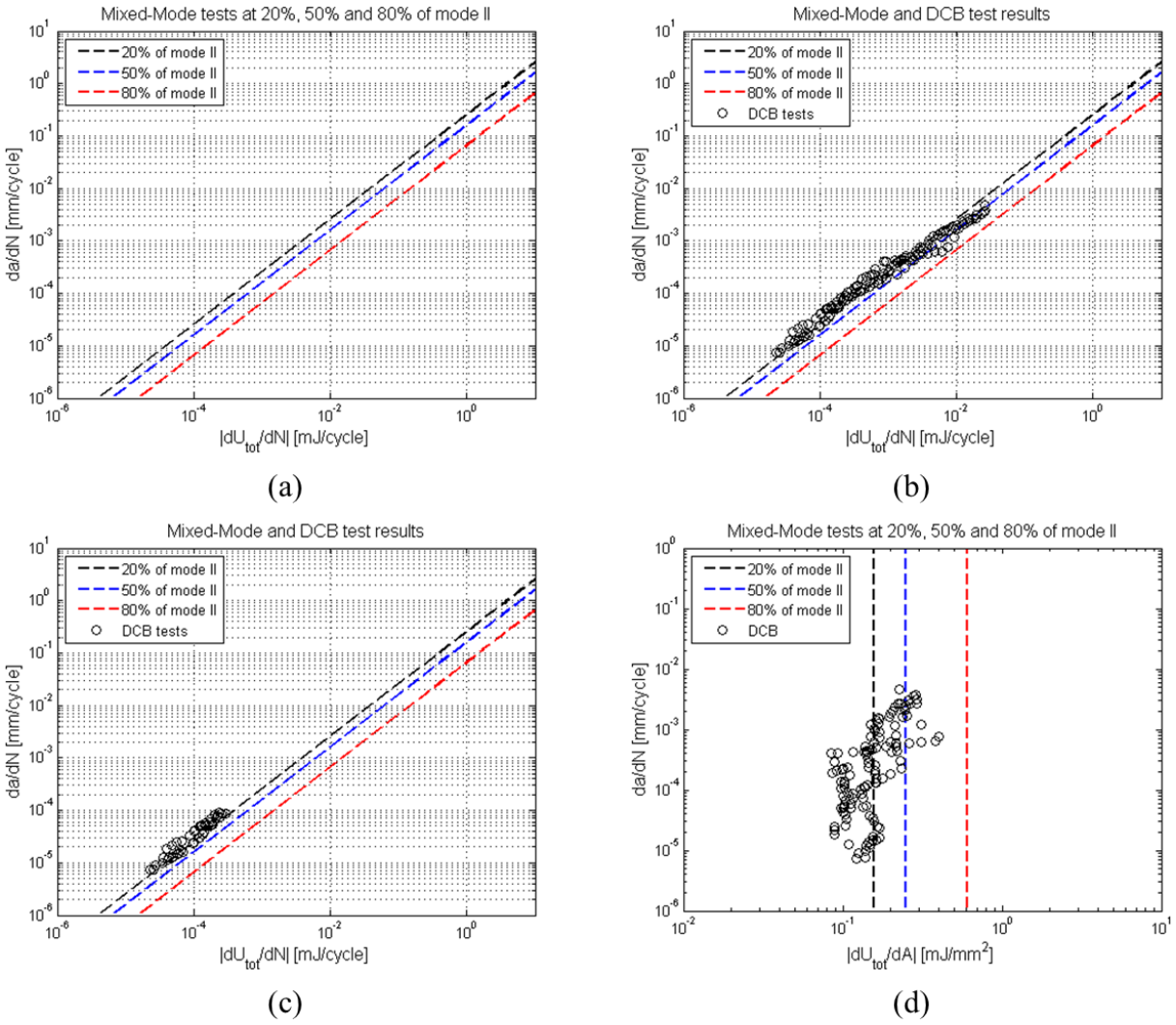

Figure 17. Trends obtained for the correlation between energy dissipation per cycle and crack growth rate for (a) mixed-mode tests, (b) mixed-mode and DCB tests and (c) mixed-mode and DCB data without breakage of bridging fibres; (d) correlation between energy dissipation per area and crack growth rate

According to what is described by Liaojun et al. [20], at crack growth rates higher than 10^{-4} *mm/cycle*, a new damage mechanism acts in mode I fatigue delamination growth for this material system: the bridging fibres break, dissipating a significant amount of energy. Figure 17 (d) shows that more energy is then released per area of crack created. The breakage of bridging fibres, activated at crack growth rates higher than 10^{-4} *mm/cycle*, increases the resistance of the specimen to delamination growth. As an example of this effect, Figure 17 (c) shows the mixed-mode test trends plotted together with the DCB data not considering the part in which the bridging fibres break. For this case, DCB data have a linear relationship between damage growth rate and energy dissipation per cycle, which is similar to the to the one for 20% of mode II loading. Similarly, the fracture surfaces for these DCB specimens at crack growth rates smaller than 10^{-4} *mm/cycle*, discussed in [15, 20], are similar to the ones presented in this work for 20% of mode II loading, which explains the similarity in delamination resistance of these data points.

For mixed-mode tests at 20% of mode II loading, bundles of broken fibres were also observed on the fracture surfaces at high crack growth rates, as shown in Figure 18 (a). However, the breakage of these bridging fibres was not dominant on the fracture surface as in [20] for pure mode I delamination. In fact, the data points in Figure 18 (b) also show that the effect of the breakage of these fibres at 20% of mode II loading was not dominant. The plot in Figure 18 (b) shows mixed-mode data at 20% of mode II loading without the points in which the breakage of bridging fibres occur for pure mode I loading, i.e., crack growth rates higher than 10^{-4} mm/cycle. However, the trend presented in this plot is the one obtained through a linear fit of the data at 20% of mode II loading shown in Figure 15 (a), in which crack growth rates higher than 10^{-4} mm/cycle were not excluded. Although the scatter is bigger at low crack growth rates, the data points presented in Figure 18 (b) still show a good agreement with the trend obtained in Figure 8 (a), showing that the effect of the breakage of these fibres can be neglected for mixed-mode tests at 20% of mode II loading.

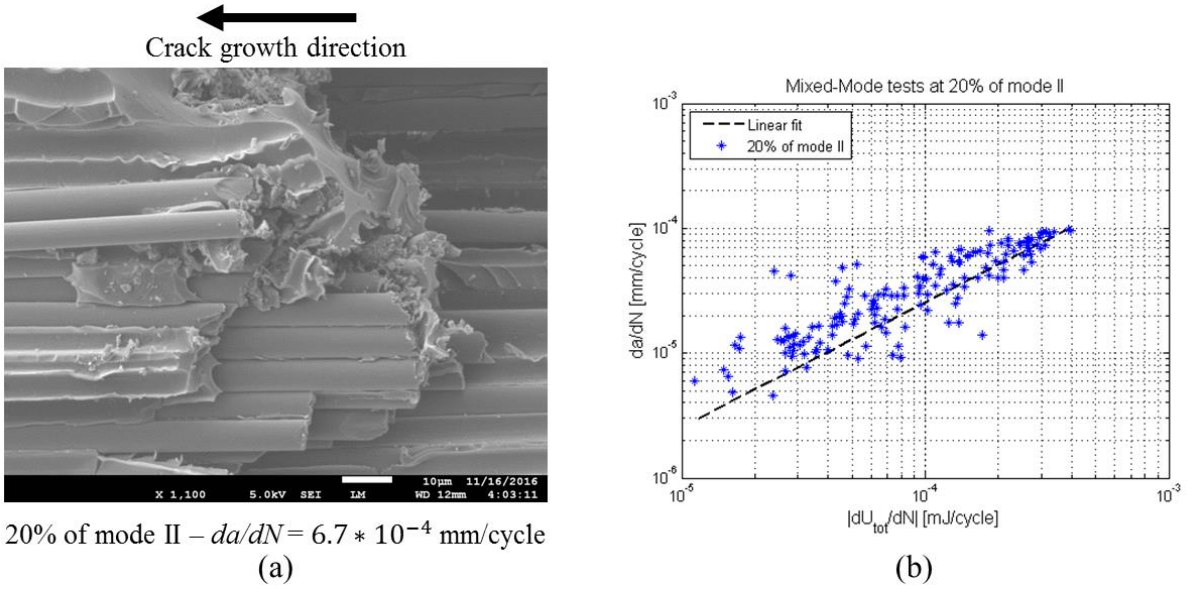

Figure 18. (a) bundle of broken fibres at high crack growth ratio – 20% of mode II loading; (b) 20% of mode II loading - test data omitting points in which crack growth rate is higher than 10^{-4} mm/cycle

3.5. The "stress ratio effect"

The use of the term "stress ratio effect" to refer to changes in delamination resistance with loading parameters is misleading. In fact, in Paris relationships the appearance of a stress ratio dependence is not connected to any physical mechanism acting in fracture. Instead, this effect of shifted Paris curves is a consequence of the way data is presented. Consider the data for 20% of mode II loading at $R_\delta=0.1$ and $R_\delta=0.5$. Figure 19 shows the measured crack growth rates plotted against G_{max} for these tests. The reader can observe that, even if the outlier present on the chart is disregarded, the curves are clearly shifted for different values of R_δ. This behaviour highlights the problems of using similitude parameters which are not based on the physics of the problem.

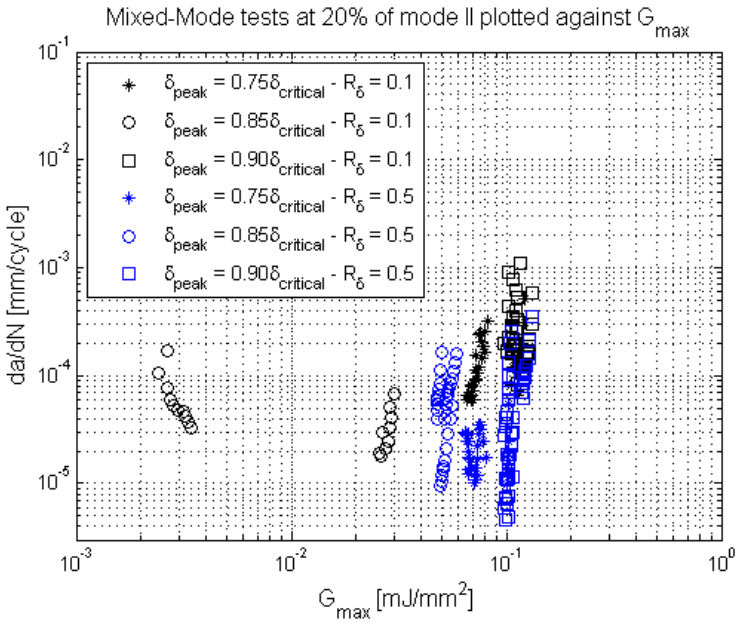

Figure 19. Mixed-mode tests performed at 20% of mode II loading – crack growth rate plotted against G_{max}

Meanwhile, consider Eq. (3), which constitutes the physics of the problem. Any stress ratio dependence on the relationship between crack growth rate and energy dissipation per cycle must be explained by the physics of damage growth.

Different dissipation mechanisms can be activated by two different loading parameters. The first parameter is the maximum displacement, as the case of the breakage of bridging fibres for pure mode I delamination growth. Meanwhile, the second parameter is the displacement ratio, as the case discussed in [17] where the formation and further coalescence of a process zone for pure mode II delamination depend on the amplitude of the fatigue loading. Therefore, even when characterizing fatigue delamination growth with a physics-based equation given by Eq. (3), one should not bluntly assert that a "stress ratio effect" must or must not be present. First, the relationship between the loading parameters and the dissipation mechanisms they activate in the given material must be known. Once these relationships are known, one can assess whether it is physically plausible to encounter different resistances to delamination under different loading parameters. Moreover, the authors reinforce that the term "stress ratio effect" is a misnomer, as discussed elsewhere [3]. The term "stress ratio effect" should not, then, be used. Scientists and engineers should, instead, refer to changes in delamination resistance due to loading parameters.

4. Conclusion

Mixed-mode delamination fatigue tests were performed at different mode mixities, displacement ratios and maximum displacements. The physical SERR G^* was used as the similitude parameter, enabling a deeper understanding of the physics behind the observed phenomena and the characterization of fatigue mixed-mode delamination propagation.

For a given mode mixity, no displacement ratio effect was observed. A higher maximum displacement leads to a higher initial crack growth rate. The energy consumed per area of crack created, however, remains approximately the same. What causes a delamination extension under a specific mode of loading to spend more energy per area of crack created are the different damage mechanisms that might be activated and the energy dissipated by plasticity under certain loading parameters. For pure mode I loading these mechanisms are the breakage of bridging fibres at high crack growth rates. Therefore, the damage features encountered on the fracture surfaces were connected to the energy dissipated on damage growth under fatigue loading. For mode II dominated delamination growth, only an approximation was possible when relating damage created and energy dissipated. This reinforces the necessity of more research into quantifying damage under mode II delamination growth.

Moreover, the term "stress ratio effect" is found to be inappropriate and misleading in case of presenting delamination resistance. With the use of the physical SERR G^*, no dependence with the displacement ratio was found when relating crack growth rate and energy dissipation per cycle. The energy dissipated per area of crack created may change with loading parameters. However, this depends on whether the different loading parameters activate different damage or dissipation mechanisms. Therefore, the existence of a physical stress ratio dependence can only be confirmed for a given material under a certain mode of loading once the relationship between the fatigue loading parameters and the dissipation mechanisms they activate is known.

5. Acknowledgements

This work was financially supported by CNPq, Conselho Nacional de Desenvolvimento Científico e Tecnológico – Brazil. Furthermore, authors would like to thank Lenny Jacquinot for performing with excellence part of the experiments reported in this paper during his internship at Delft University of Technology.

6. References

[1] Hojo M, Ando T, Tanaka M, Adachi T, Ochiai S, Endo Y. Modes I and II interlaminar fracture toughness and fatigue delamination of CF/epoxy laminates with self-same epoxy interleaf. International Journal of Fatigue. 2006;28:1154-65.
[2] Hojo M, Ochiai S, Gustafson C-G, Tanaka K. Effect of matrix resin on delamination fatigue crack growth in CFRP laminates. Engineering Fracture Mechanics. 1994;49:35-47.
[3] Pascoe JA, Alderliesten RC, Benedictus R. Methods for the prediction of fatigue delamination growth in composites and adhesive bonds - A critical review. Engineering Fracture Mechanics. 2013;112-113:72-96.
[4] Jones R, Stelzer S, Brunner AJ. Mode I, II and Mixed Mode I/II delamination growth in composites. Composite Structures. 2014;110:317-24.
[5] Reeder JR, Crews J. Redesign of the mixed-mode bending delamination test to reduce nonlinear effects. Journal of Composites, Technology and Research. 1992;14:12-9.

[6] Gustafson C-Go, Hojo M. Delamination Fatigue Crack Growth in Unidirectional Graphite/Epoxy Laminates. Journal of Reinforced Plastics and Composites. 1987;6:36-52.
[7] Zhang J, Peng L, Zhao L, Fei B. Fatigue delamination growth rates and thresholds of composite laminates under mixed mode loading. International Journal of Fatigue. 2012;40:7-15.
[8] Blanco N, Gamstedt EK, Asp LE, Costa J. Mixed-mode delamination growth in carbon-fibre composite laminates under cyclic loading. International Journal of Solids and Structures. 2004;41:4219-35.
[9] Zhao S, Gadke M, Prinz R. Mixed-Mode Delamination Behavior of Carbon/Epoxy Composites. Journal of Reinforced Plastics and Composites. 1995;14:804-26.
[10] Asp LE, Sjögren A, Greenhalgh ES. Delamination growth and thresholds in a carbon/epoxy composite under fatigue loading. Journal of Composites, Technology and Research. 2001;23:55-68.
[11] Rans C, Alderliesten RC, Benedictus R. Misinterpreting the results: How similitude can improve our understanding of fatigue delamination growth. Composites Science and Technology. 2011;71:230-8.
[12] Jones R, Kinloch AJ, Hu W. Cyclic-fatigue crack growth in composite and adhesively-bonded structures: The FAA slow crack growth approach to certification and the problem of similitude. International Journal of Fatigue. 2016;88:10-8.
[13] Roderick GL, Everett RA, Crews Jr JH. Debond Propagation in Composite Reinforced Metals. Hampton, VA: NASA; 1974.
[14] Mostovoy S, Ripling EJ. Flaw Tolerance of a Number of Commercial and Experimental Adhesives. In: Lee L-H, editor. Adhesion Science and Technology. New York: Plenum Press; 1975. p. 513-62.
[15] Amaral L, Yao L, Alderliesten R, Benedictus R. The relation between the strain energy release in fatigue and quasi-static crack growth. Engineering Fracture Mechanics. 2015;145:86-97.
[16] Alderliesten RC. How proper similitude can improve our understanding of crack closure and plasticity in fatigue. International Journal of Fatigue. 2016;82, Part 2:263-73.
[17] Amaral L, Zarouchas D, Alderliesten R, Benedictus R. Energy dissipation in mode II fatigue crack growth. Engineering Fracture Mechanics. 2017;173:41-54.
[18] Pascoe JA, Alderliesten RC, Benedictus R. Towards Understanding Fatigue Disbond Growth via Cyclic Strain Energy. Procedia Materials Science 2014;3 (ECF-20):610-5.
[19] Pascoe JA, Alderliesten RC, Benedictus R. On the relationship between disbond growth and the release of strain energy. Engineering Fracture Mechanics. 2015;133:1-13.
[20] Yao L, Alderliesten R, Benedictus R. Interpreting the stress ratio effect on delamination growth in composite laminates using the concept of fatigue fracture toughness. Submitted to Composites: Part A. 2015.
[21] Yao L, Alderliesten RC, Zhao M, Benedictus R. Discussion on the use of the strain energy release rate for fatigue delamination characterization. Composites Part A: Applied Science and Manufacturing. 2014;66:65-72.
[22] Griffith AA. The Phenomena of Rupture and Flow in Solids. Philosophical Transactions of the Royal Society of London Series A, Containing Papers of a Mathematical or Physical Character. 1921;221:163-98.
[23] ASTM Standard D 6671/ D 6671M-06. Standard Test Method for Mixed Mode I-Mode II Interlaminar Fracture Thoughness of Unidirectional Fiber Reinforced Polymer Matrix Composites. US: ASTM International; 2006.
[24] Rodi R. The residual strength failure sequence in fibre metal laminates: TU Delft, Delft University of Technology; 2012.
[25] ASTM. Standard Test Method for Measurement of Fatigue Crack Growth Rates. E647-15: ASTM International; 2015.
[26] Amaral L, Yao L, Alderliesten RC, Benedictus R. Energy based study on quasi-static delamination growth treated as a low cycle fatigue process. In: Siljander A, editor. 34th Conference and 28th Symposium of the International Committee on Aeronautical Fatigue and Structural Integrity. Helsinki, Finland2015. p. 240 - 8.

[27] Amaral L, Alderliesten RC, Benedictus R. Towards the Fundamentals of Mode II Fatigue Delamination Growth. 31st Technical Conference of the American Society for Composites. Williamsburg, Virginia, USA2016.
[28] Corleto C, Bradley W. Mode II Delamination Fracture Toughness of Unidirectional Graphite/Epoxy Composites. Composite Materials: Fatigue and Fracture. 1989;2:201-21.
[29] Greenhalgh ES. Failure analysis and fractography of polymer composites: Woodhead Publishing Limited; 2009.
[30] LEE SM. Mode II delamination failure mechanisms of polymer matrix composites. Journal of Materials Science. 1997;32:1287-95.
[31] Lee SM. Mode II Interlaminar Crack Growth Process in Polymer Matrix Composites. Journal of Reinforced Plastics and Composites. 1999;18:1254-66.